Kalpa Publications in Computing

Volume 22, 2025, Pages 1164–1174

Proceedings of The Sixth International Conference on Civil and Building Engineering Informatics

Real-time On-site Indoor Modeling and Quality Visualization using Mixed Reality Device with TOF Sensor

Norihiko Goto[1], Hiroaki Date[1] and Satoshi Kanai[1]

[1] Hokkaido University

hdate@ist.hokudai.ac.jp

Abstract

In this study, we propose a real-time on-site indoor modeling method and a modeling quality visualization method that use a mixed reality (MR) device with a time-of-flight (ToF) sensor to realize efficient and reliable indoor model generation. The modeling method is based on rule-based fast voxel labeling and consists of two steps: local and global modeling. In the local modeling, space occupancy labels and attribute labels (ceiling, wall, wall opening, wall candidate, floor, object, and space) are assigned to each cell of the local voxel from point clouds in each frame of laser scanning by the MR device. In global modeling, the results of the local modeling are integrated with the global voxel, considering the label assignment quality based on entropy and probability. The quality of the resulting model is presented to the user through MR visualization to verify the modeling results. For real-time visualization of the quality of the modeling results, a simple textured polygon model is created and used for MR visualization. The polygon model is efficiently generated from the local and global voxels, and the texture represents the quality of the modeling results. Our method was applied to a real indoor environment and its performance was evaluated. The modeling frame rate was 2 fps, and the labeling precision was 98%. A polygon model for MR visualization was created and updated within 20 msec, and real-time MR visualization was achieved. These results show that real-time indoor modeling and on-site quality checks using an MR device with a ToF sensor can be realized.

1 Introduction

Three-dimensional (3D) scanning technologies for large-scale environments and structures have been rapidly developed over the past decade and are used in a wide range of fields, including plant engineering, surveying, architecture, civil engineering, forests, and construction. Laser scanning and image-based 3D reconstruction techniques allow us to acquire point clouds or meshes of real

I. Hkust, J. Cheng and Y. Yantao (eds.), ICCBEI 2025 (Kalpa Publications in Computing, vol. 22), pp. 1164–1174

environments and structures, and several types of platforms are available, such as drones/vehicles for large outdoor areas and terrestrial/backpack/handheld platforms for indoor environments and large-scale structures. Recently, time-of-flight (ToF) sensors have been installed in handheld mobile devices and head-mounted mixed reality (MR) devices. MR devices are especially suited for interactive and real-time applications because of their ability to acquire and show 3D geometric information in both cyber and physical spaces.

With the advancement of 3D scanning technology, many methods for modeling indoor environments have been developed and used in practical applications. The 3D model of the indoor environment based on 3D scanning technology has many applications in fields such as maintenance, drawing generation, navigation, simulation, planning, and MR. Many studies on 3D indoor modeling and recognition from point clouds acquired by laser scanning have been conducted (Akiyama et al., 2024; Cui et al., 2023; Hübner et al., 2021; Macher et al., 2017; Martens & Blankenbach, 2023; Monszpart et al., 2015; Pan et al., 2022; Qi et al., 2017; Quintana et al., 2018; Takahashi et al., 2019). The targets of modeling and recognition are indoor structures such as rooms, ceilings, walls, floors (Cui et al., 2023; Macher et al., 2017; Martens & Blankenbach, 2023), doors (Quintana et al., 2018), windows (Takahashi et al., 2020), and small facilities (Akiyama et al., 2024; Giovanni et al., 2018; Pan et al., 2022). In addition to the rule- or algorithm-based methods, machine-learning-based methods have become widely used (Qi et al., 2017). To realize accurate and efficient reconstruction, Manhattan assumptions and regularities are available (Monszpart et al., 2015; Takahashi et al., 2019). Recently, speed-specific algorithms that use voxels have been proposed (Hübner et al., 2021; Martens & Blankenbach, 2023).

The modeling of indoor environments based on 3D scanning is often performed offline after the scanning operation has been completed on-site and point clouds of the entire environment have been acquired. However, in this approach, it is difficult to guarantee the quality of the point clouds and the resulting 3D models. Point clouds from scanning often have problems related to density, scanning errors, and lack of points owing to occlusions; therefore, in the worst case, additional scanning may be required back on-site. To solve these problems, we propose a real-time on-site indoor reconstruction and quality check method using an MR device with a ToF sensor. Figure 1 shows an outline of the proposed method. This method consists of real-time voxel-based indoor modeling and MR visualization of the quality of the modeling results. The scanning of the environment is performed by the MR device at approximately 5 fps while walking and seeing the environments (Figure 1(i)), and voxel models of the indoor reconstruction are generated using the rule-based method in real-time (Figure 1(ii)). The modeling is realized using the point cloud for each frame, and the results are successively merged with previous results. The quality of the modeling is shown to the user using on-site MR visualization (Figure 1(iv)). To realize efficient MR visualization, a method for generating a simple textured polygon model that can represent the quality of the indoor reconstruction is developed (Figure 1(iii)).

The details of the proposed method are described in Section 2, and the experimental results and discussions are presented in Section 3.

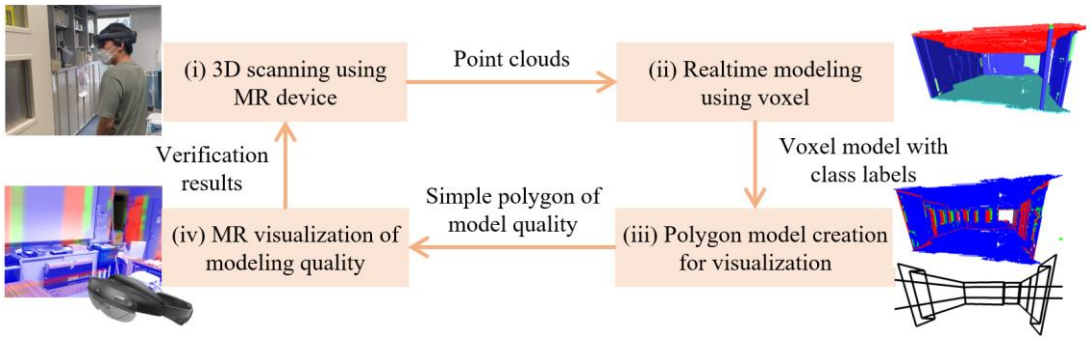

Figure 1: The proposed real-time on-site indoor modeling and quality visualization method using a mixed reality (MR) device

2 Method

2.1 Mixed Reality Device and Method Overview

The input for this method consists of a series of point clouds acquired using a head-mounted MR device. A Microsoft HoloLens2 (Microsoft, 2024) is used in this study. The device mounts a ToF LiDAR sensor, and real-time point cloud acquisition at approximately 5 fps is realized. The point cloud per frame contains approximately 60,000 points. Each point has a unit normal vector, and the measurement range is approximately 3.5 m. The point cloud in each frame is automatically registered using the self-localization function of the device in a global coordinate system.

In this study, a real-time modeling method for point clouds acquired from MR devices and an MR visualization method of the quality of the modeling results are developed. The flow of the proposed method is illustrated in Figure 2. The output of the modeling method is an indoor reconstruction voxel model, in which one of the attribute labels is assigned to each cell. Similar to the existing method (Hübner et al., 2021), the attribute labels include *ceiling*, *wall*, *wall_opening*, *wall_candidate*, *floor*, *object*, and *space*. The *wall_opening* label corresponds to the entrances of a room or windows. The *wall_candidate* label represents the candidates for a wall, such as the regions occluded by a shelf in front of a wall. The proposed indoor modeling method consists of local modeling, which generates a local voxel with labels assigned from a point cloud in a frame, and global modeling, which integrates the labels from the local modeling and updates some labels that cannot be estimated in only one frame (Figure 2, A-1,2). As different labels may be assigned to the same cell of a global voxel in the local modeling, a measure of the reliability of the label is calculated during the integration process to evaluate the quality of the resulting model. In contrast to common modeling approaches (Hübner et al., 2021; Martens & Blankenbach, 2023), this method creates a voxel model immediately while acquiring the point clouds to provide online feedback on the modeling results and their quality to the user with the MR device.

The MR device allows us to superimpose 3D digital information onto the real world using MR visualization. Because the user is always on-site during scanning, we try to show the modeling results and their quality to the user on-site and in real-time utilizing MR. Unfortunately, voxel models and point clouds are not appropriate for MR visualization because of the large amount of data. Therefore, a 3D model suitable for MR visualization of modeling quality is proposed. In this study, a simple polygon with texture is used and an efficient generation method is proposed for our modeling framework (Figure 2, A-3).

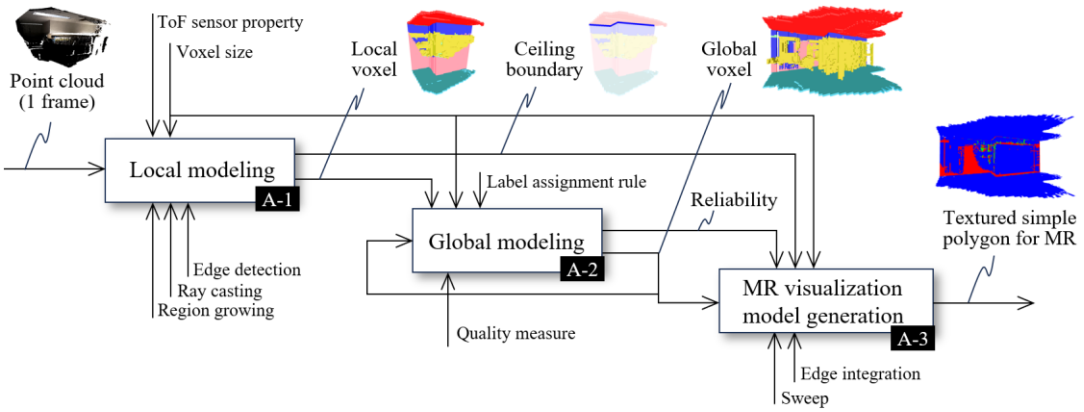

Figure 2: A flow of voxel-based modeling and MR model generation

2.2 Voxel-based Indoor Modeling

(1) Definition and Assumptions

Figure 3(a) shows a scene and the definitions of certain terms. Our modeling method is based on the following observations and properties of each entity: The ceiling is a large plane with a downward normal above the device (ToF sensor) position. The floor is a large plane with an upward normal below the device position. The walls are vertical planes below the ceiling boundary. The region on a wall plane through which the laser passes is recognized as a wall opening. The objects are represented by the scanned points between the ceiling and the floor, and free space is recognized as the region through which the laser passes during laser scanning. The occluded regions can be detected by ray casting from the device position to points in the point cloud, and the vertical occluded region below the ceiling boundary is recognized as an occluded wall. The occluded floor can be estimated by interpolation/extrapolation at the floor height within the ceiling range. This method assumes that the floor and ceiling heights of the environment to be reconstructed are constant. In the coordinate system of the point clouds and modeling, the vertical direction corresponds to the z-axis.

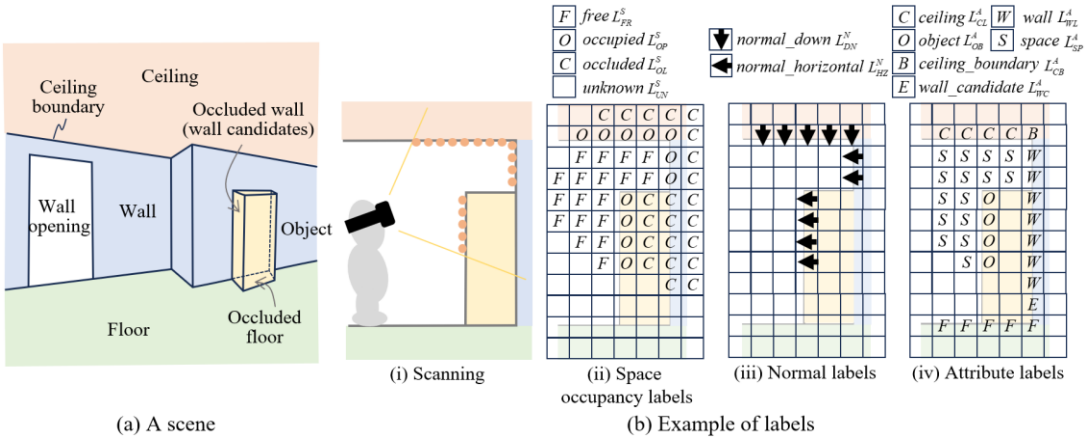

Figure 3: A scene and an example of labels

(2) Local Modeling

Local modeling consists of three steps: initial voxel generation, floor/ceiling detection, and wall/object detection. First, the initial voxel with space occupancy and normal labels is generated (Figure 3 (b) (ii)-(iii)). Next, the ceiling, ceiling boundaries, and the floor are detected based on the normal labels. Finally, walls, wall openings, wall candidates, objects, and spaces are detected from the ceiling information (Figure 3 (b) (iv)). The basic labeling strategy for the ceiling and walls is based on an existing method (Hübner et al., 2021), but the method is simplified to realize real-time labeling for a one-frame point cloud. In addition, by using ray casting, reliable estimation of occluded regions and labeling are achieved using our method.

During the initial voxel generation, a voxel with space occupancy and normal labels is generated. First, a voxel grid is defined by uniformly dividing the space of the scanner's measurement range (3.5 m for HoloLens2) using a specified voxel size. The voxel size is set to 5 cm in our implementation, according to the accuracy of the point clouds from the experiments. The center of the voxel space is the device position. Then, using the ray casting from the device position in the voxel space, the space occupancy label, *occupied* L^S_{OP}, *unknown* L^S_{UN}, *free* L^S_{FR}, or *occluded* L^S_{OL}, is assigned to each cell as shown in Figure 3(b) (ii). In this process, L^S_{UN} is first assigned to all cells, and L^S_{OP} is assigned to the cells containing the points. L^S_{FR} and L^S_{OL} are then assigned using ray casting from the device position to the cells within the scanner's field of view and measurement range. Finally, in each cell c with L^S_{OP}, the unit average normal vector $\mathbf{n}_c = (x_{nc}, y_{nc}, z_{nc})$ of the points in it is calculated. For the fast computation of region detection, normal information is classified into three types and labeled in the voxel. The label *normal_up* L^N_{UP}, *normal_down* L^N_{DN}, or *normal_horizontal* L^N_{HZ} is assigned as the normal label l_c of cell c according to Equation (1), where τ_c is a given threshold (0.75 is used in the experiments).

$$l_c = \begin{cases} L^N_{UP} & (z_{nc} > \tau_n) \\ L^N_{DN} & (z_{nc} < -\tau_n) \\ L^N_{HZ} & (otherwise) \end{cases} \tag{1}$$

In floor/ceiling detection, the floor and ceiling regions are detected quickly from the initial voxel. In this process, the attribute labels of *ceiling* L^A_{CL}, *ceiling_boundary* L^A_{CB}, and *floor* L^A_{FL} are assigned, and the height of the floor h_f is calculated. The ceiling region is defined as a set of more than a certain number of connected L^N_{DN} cells above the device position. The connected L^N_{DN} cells are detected by using region growing (Poux et al., 2022). When a ceiling region is detected, the boundaries of the ceiling region are recognized as its boundary cells that have L^N_{HZ} cells below them. An example of this labeling is shown in Figure 3(b) (iv). On the other hand, the floor region is detected as a set of more than a certain number of connected L^N_{UP} cells below the device position using region growing. If a floor region is detected from the point cloud once, its average height value h_f is computed and no further floor detection processing is performed, and the label of *floor* L^A_{FL} is assigned to the cells at height h_f under the ceiling cells.

In wall/object detection, a downward traversal is performed from the L^A_{CL} (*ceiling*) and L^A_{CB} (*ceiling_boundary*) cells to the floor level h_f. According to the space occupancy labels of the visited cells in the traversal, *wall* L^A_{WL}, *wall_opening* L^A_{WO}, *wall_candidate* L^A_{WC}, *object* L^A_{OB}, or *space* L^A_{SP} are assigned according to the rules shown in Table 1. For example, the attribute label of a cell with an occupied label under the ceiling is *object* L^A_{OB}, and the label of a cell with an occluded label under the ceiling boundary is *wall* L^A_{WL}. For the cells at the floor level under the *ceiling* and *ceiling_boundary* cells, the *floor* label L^A_{FL} is assigned. Examples of the labeling results for a scan are shown in Figure 3(b) (iv). This label assignment process is performed when a floor has been detected

at least once and a ceiling is detected in the current point cloud.

An attribute label of the start cell of traversal	A space occupancy label of the visited cell			
	occupied L^S_{OP}	*free* L^S_{FR}	*occluded* L^S_{OL}	*unknown* L^S_{UN}
ceiling L^A_{CL}	*object* L^A_{OB}	*space* L^A_{SP}	–	–
ceiling_boundary L^A_{CB}	*wall* L^A_{WL}	*wall_opening* L^A_{WO}	*wall* L^A_{WL}	*wall_candidate* L^A_{WC}

Table 1: Attribute label assignment rule

(3) Global Modeling

The space occupancy and attribute labels of the local voxels are transferred to the corresponding cells in the global voxel. First, an initial global voxel is generated by dividing a sufficiently large space with a specified voxel size (5 cm in our implementation) centered at the device position of the first frame of the point cloud acquisition. After each local voxel generation, the label of the global voxel is successively updated. In the experiments, different local voxel labels were often assigned to a cell of the global voxel because of the scanning noise and outliers in the point cloud, different scan directions, and voxel discretization errors. Therefore, in this study, a labeling method based on the reliability of labels from the local voxels is introduced.

For each cell in the global voxel, the reliability is calculated if the minimum number of the assigned labels from the local voxel is satisfied. In our study, the state probability in Equation (2) and entropy in Equation (3) are evaluated.

$$P_c^l = \frac{B_c^l}{B_c} \tag{2}$$

$$E_c = -\sum_{l \in L} P_c^l \log P_c^l \tag{3}$$

Where, B_c^l is the number of assignments of label l from the local voxel for cell c in the global voxel, B_c is the total number of label assignments for cell c, and L is the attribute-label set. A smaller entropy means that the label distribution is non-uniform, and the number of assignments of a label becomes higher compared with that of other labels, that is, the reliability of the label with the highest state probability is high. Therefore, in this method, if the entropy becomes lower than the given threshold τ_E, the attribute label l_c of the global cell is assigned using Equation (4).

$$l_c = \arg\max_{l \in L} P_c^l \tag{4}$$

2.3 Mixed Reality Visualization of Modeling Quality

A method to show the modeled regions and the quality of the modeling results and to support the additional scanning of the user in real-time using MR is proposed. Because voxel models and point clouds with large data volumes are not suitable for MR visualization from the viewpoint of data amount (Ohno et al., 2022), a simplified polygon model with texture is used. In this method, a polygon model for MR visualization is generated from the local and global voxels. The polygon model is defined by large rectangles for the ceiling and floor and rectangles for walls defined by each ceiling boundary edge, as shown in Figure 4 (right). The reconstruction results and their reliability

information are represented by texture colors. The texture color is assigned according to the entropy defined by Equation (3), and the non-reconstructed areas are transparent.

Figure 4 presents an overview of the polygon model generation method for MR visualization. The ceiling and floor polygons can be defined using large horizontal rectangles when their heights are determined. Wall polygons are created by sweeping the straight ceiling boundary edges to the floor height. In this method, the ceiling boundary edges are detected in the local modeling step. The edges detected first are directly copied to and stored in the global voxel and are updated by the edges from successive local modeling.

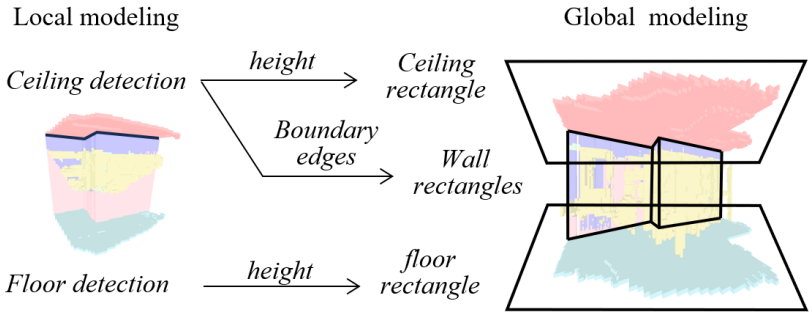

Figure 4: Polygon model generation for MR visualization

The straight-line segments of the ceiling boundary edges, which represent the boundary between the ceiling and walls, are detected by line fitting to the points in the ceiling boundary cells. For a fast computation, the barycenter points of the scanned points in each cell are used. Straight lines are detected using RANSAC (Fishler & Bolles, 1981; Schnabel et al., 2007), and the barycenter points in the cells of the endpoints of the detected lines are used as endpoints of the straight-line segments. The initial line segments from the local modeling are used as the initial line segments in the global voxel. If the new edges from the local modeling overlap with and have the same direction for the current line segments in the global voxel, the positions of the endpoints in the global voxel are modified. Otherwise, the edges are added as new edges to the global voxel. This process is performed during global modeling.

For each polygon, a texture image with a pixel size equal to the cell size of the voxel is generated. From each pixel p in the texture image, the cell c_p of the corresponding global voxel is found, and the color of p is determined based on the value of the entropy of c_p. As it is difficult to distinguish slight changes of color in MR visualization, three colors are assigned in our implementation: blue for high quality, green for medium quality, and red for low quality or for an insufficient number of labeling from the local voxel. The quality becomes higher when the scanning times are increased; therefore, red regions are identified as regions that require additional scans. Transparency is assigned to the pixels that correspond to the *wall_opening* cells or cells without the attribute labels.

3 Results and Discussions

The proposed method was applied to a room with an area of approximately 70 m^2 as shown in Figure 5(a). Scanning was performed for approximately 2 min while walking around the room. During the scanning, 607 frames and approximately 30 million points were acquired, as shown in Figure 5(b). In the experiment, to verify the feasibility of real-time modeling and polygon generation for MR visualization, voxel modeling and polygon model generation were performed using a desktop

PC with a Ryzen 5600X CPU after acquiring all the point clouds.

Figure 5(c) shows the voxel model of the resulting indoor reconstruction. The results indicated that walls, floors, ceilings, and objects were recognized and represented by the voxel model. Figure 6 shows the results of local and global modeling for each frame. The top figures in each figure show the results of the local modeling, and the middle figures show the results of global modeling. In local modeling, indoor environments are recognized from the point cloud of one frame, and the global modeling generates the integrated voxel model from the local modeling. The processing times for local and global modeling were approximately 0.5 s per frame. The acquisition rate of the point cloud was 5 fps, and real-time processing reflecting the acquired point cloud was possible for every two or three frames. In our framework, local modeling can also be performed using parallel processing to improve the modeling frame rate, which will be included in future work.

(a) A room for experiments (b) Acquired point clouds (left: exterior view, right: inside view)

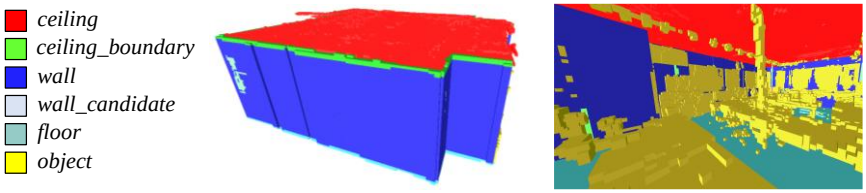

(c) Resulting voxel model (middle: exterior view, right: inside view)

Figure 5: Point clouds and voxel modeling results

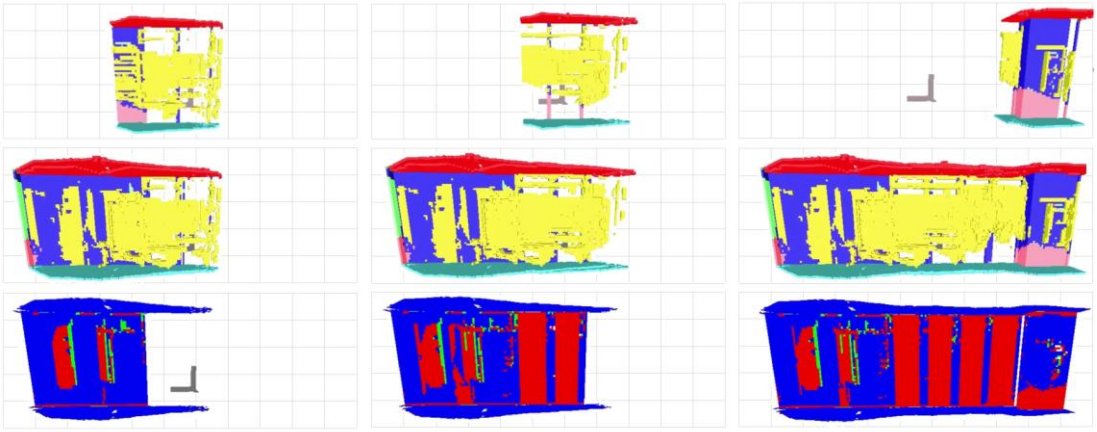

(a) 10 frame (b) 20 frame (c) 40 frame

Figure 6: Local voxels, global voxels, and MR models for different frames (top: local modeling results, middle: global modeling results, bottom: textured polygon models for MR visualization of modeling quality)

To confirm the accuracy of the generated voxel model, a ground truth model with the walls, floor, and ceiling of the room was generated by accurate laser scanning using a terrestrial laser scanner and

a manual modeling operation using 3D modeling software (Blender). The ground truth model and the results reconstructed by our method were registered, and the precision was evaluated. Adjacent cells were also considered correct in the evaluation to mitigate the effects of discretization and registration errors. The precision of labeling the global voxel was approximately 98%, and it was confirmed that accurate 3D modeling could be performed using our method.

The bottom figures in Figure 6 show the textured polygon models used to visualize the reconstruction quality for each frame. Only the walls, floors, and ceilings are shown in each figure. The results show that the textured model adequately represents the quality of the global modeling of the walls, floors, and ceilings. The quality of the wall is low in some regions where the labeling is unstable or where labels are not assigned because of tall bookshelves that make ceiling boundary estimation difficult. Figure 7 shows a wireframe representation of the polygon model. A simple polygon model is generated. The textured polygon model was generated at 20 ms per frame, which was sufficient for real-time processing. Figure 8 shows the MR visualization results of the textured polygon model. The MR visualization could be performed at a high frame rate, and the simple textured polygon model was effective in showing the modeling quality on-site using MR.

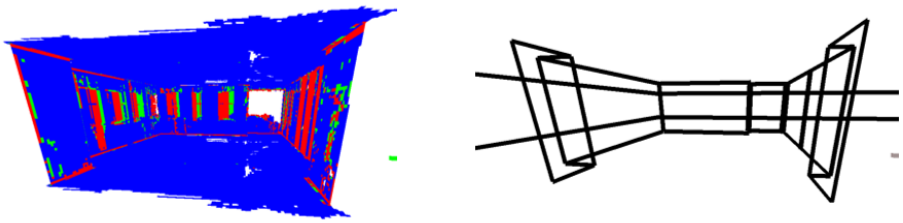

(a) Textured polygon model (b) Wireframe representation of polygons

Figure 7: Textured polygon model and wireframe representation of polygons

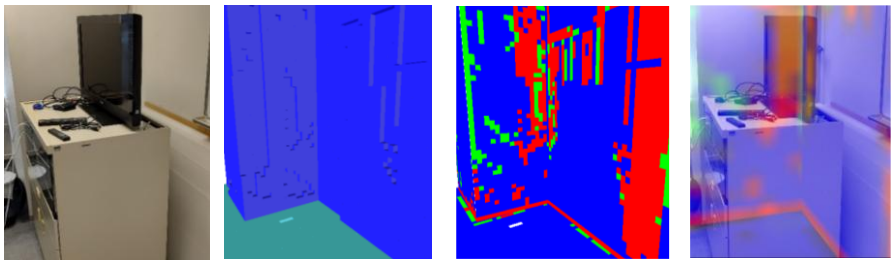

Photo Global voxel Textured polygon MR visualization

(a) Correctly reconstructed occluded region

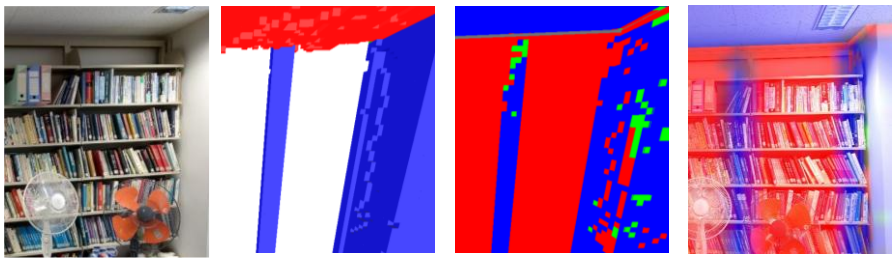

Photo Global voxel Textured polygon MR visualization

(b) Unreconstructed walls caused by large occlusion

Figure 8: MR visualization of modeling quality

The proposed method assumes that the indoor environments have a horizontal ceiling. In addition, sufficient measurement of the ceiling boundary leads to an accurate reconstruction model. Real environments may include sloped ceilings, cases where the ceiling boundary is occluded by tall objects, and objects or structures that are difficult to scan, such as glass doors. The development of a method for applying complex environments by using regularity recognition and beautification (Takahashi et al., 2019), and image-based recognition is included in the future works.

4 Conclusions

In this study, a real-time on-site indoor modeling method based on fast voxel labeling and a quality visualization method based on simple textured polygons using an MR device with a ToF sensor are proposed. The modeling method consists of a local modeling method that rapidly assigns labels such as walls, floors, and ceilings from the point cloud in each frame and a global modeling method that integrates the results of the local modeling considering the quality of labeling based on the entropy and state probability. For quality visualization, a method for generating simple textured polygon models is proposed.

The experimental results showed that indoor reconstruction could be performed at 2 fps with a labeling precision of 98%. These results demonstrate the capability of real-time voxel modeling using point clouds acquired by an MR device. In addition, polygon models for MR visualization can be generated and updated within 20 ms, and MR visualization using polygons can be performed at a high frame rate. The MR display of the reconstruction quality was found to intuitively convey areas that were well reconstructed and those that were difficult to measure and not well reconstructed.

Future work will include the implementation of a server-client system to transfer the acquired point clouds and the 3D polygon model wirelessly between the MR device and a computer for modeling and the application to large-scale and complex indoor environments.

Acknowledgments

This work was supported by JSPS KAKENHI Grant Number JP24K01044.

References

Akiyama, R., Date, H., Kanai, S., and Yasutake, K. (2024). Ceiling Equipment Extraction from TLS Point Clouds for Reflected Ceiling Plan Creation, *International Journal of Automation Technology*, 18 (5), 603-612.

Cui, Y., Yang, B., Liu, P., and Kong, L. (2023). A Review of Indoor Automation Modeling Based on Light Detection and Ranging Point Clouds, *Sensors and Materials*, 35 (1), 247-268.

Fischler, M. A. and Bolles, R. C. (1981). Random Sample Consensus: A paradigm for model fitting with applications to image analysis and automated cartography, *Communications of the ACM*, 24 (6), 381-395.

Giovanni, P., Ruggero, P., Fabio, G., Roberto, S., and Enrico, G. (2018). Recovering 3D existing-conditions of indoor structures from spherical images, *Computers & Graphics*, 77, 16-29.

Hübner, P., Weinmann, M., Wursthorn, S, and Hinz, S. (2021). Automatic voxel-based 3D indoor reconstruction and room partitioning from triangle meshes, *ISPRS Journal of Photogrammetry and Remote Sensing*, 181, 254-278.

Macher, H., Landes, T., and Grussenmeyer, P. (2017). From Point Clouds to Building Information Models: 3D Semi-Automatic Reconstruction of Indoors of Existing Buildings, *Applied Sciences*, 7, 1030.

Martens, J. and Blankenbach, J. (2023). VOX2BIM+ - A Fast and Robust Approach for Automated Indoor Point Cloud Segmentation and Building Model Generation, *Journal of Photogrammetry, Remote Sensing and Geoinformation Science*, 91, 273-294.

Microsoft HoloLens2. (2024). website: https://www.microsoft.com/ja-jp/hololens

Monszpart, A., Mellado, N., Brostow, G. J., and Mitra, N. J. (2015). RAPter: rebuilding man-made scenes with regular arrangements of planes, *ACM Transactions on Graphics*, 34 (4), Article No 103.

Ohno, K., Date, H., and Kanai, S. (2022). MIXED REALITY VISUALIZATION OF POINT CLOUDS FOR SUPPORTING TERRESTRIAL LASER SCANNING, *The International Archives of the Photogrammetry Remote Sensing and Spatial Information Sciences*, XLIII-B2-2022, 251-258.

Pan,Y., Braun, A., Brilakis, I., and Borrmann, A. (2022). Enriching geometric digital twins of buildings with small objects by fusing laser scanning and AI-based image recognition, *Automation in Construction*, 140, 104375.

Poux, F., Mattes, C., Selman, Z., and Kobbelt, L. (2022). Automatic region-growing system for the segmentation of large point clouds, *Automation in Construction*, 138, 104250.

Qi, C. R., Yi, L., Su, H., and Guibas, L. J. (2017). PointNet++: Deep Hierarchical Feature Learning on Point Sets in a Metric Space, In *Proceedings of the 31st International Conference on Neural Information Processing Systems*, 5105-5114.

Quintana, B., Prieto, S.A., Adán, A., and Bosché, F. (2018). Door detection in 3D coloured point clouds of indoor environments, *Automation in Construction*, 83, 146-166.

Schnabel, R., Wahl, R., and Klein, R. (2007). Efficient RANSAC for Point-Cloud Shape Detection, *Computer Graphics Forum*, 26 (2), 214-226.

Takahashi, H., Date, H., and Kanai, S. (2019). Automatic Indoor Environment Modeling from Laser-scanned Point Clouds Using Graph-Based Regular Arrangement Recognition, In *Proceedings of the 4th International Conference on Civil and Building Engineering Informatics*, 368-375.

Takahashi, H., Date, H., Kanai, S., and Yasutake, K. (2020). DETECTION OF INDOOR ATTACHED EQUIPMENT FROM TLS POINT CLOUDS USING PLANAR REGION BOUNDARY, *The International Archives of the Photogrammetry Remote Sensing and Spatial Information Sciences*, XLIII-B2-2020, 495-500.